Contrib. Astron. Obs. Skalnaté Pleso **56/1**, 15 – 30, (2026)
https://doi.org/10.31577/caosp.2026.56.1.15

Exploring the broad-line region of PKS 1510-089: Jet contributions and mass estimation

A. Amador-Portes[1], **A. García-Pérez**[1,2], **V. Chavushyan**[1] **and V.M. Patiño-Álvarez**[1,3]

[1] *Instituto Nacional de Astrofísica, Óptica y Electrónica, Luis Enrique Erro 1, Tonantzintla Puebla, México, C.P. 72840 (E-mail: alfreportess9730@gmail.com)*

[2] *Dipartimento di Fisica, Università degli Studi di Torino, via Pietro Giuria 1, I-10125 Torino, Italy*

[3] *Max-Planck-Institut für Radioastronomie, Auf dem Hügel 69, D-53121 Bonn, Germany*

Received: August 5, 2025.; Accepted: November 12, 2025.

Abstract.

PKS 1510-089, a highly active flat-spectrum radio quasar, known for its frequent flaring activity across the electromagnetic spectrum. We present a decade-long analysis of its flux variability in optical bands and γ-rays, focusing on the non-thermal dominance parameter, Hβ and Hγ lines, and the λ5100 Å continuum. We examine the Hβ flux and full width at half maximum (FWHM), along with the λ5100 Å continuum light curves to assess whether the primary source of continuum emission is the accretion disk or the jet during different activity periods. Our results highlight that jet emission dominates the continuum during flare-like episodes. We obtain an approximately 80 day delay between the Hβ and continuum emissions, which we interpret as the spatial separation between the optical emission region and the broad-line region (BLR). Near-zero delays between optical and near-infrared bands indicate co-spatial emission within the jet. Synchrotron self-Compton is identified as the dominant γ-ray mechanism during flares, supported by minimal delays with optical/NIR emission. A persistent anticorrelation between the Hβ FWHM and luminosity reveals a "breathing-BLR" effect, independent of whether ionization arises from the disk or jet. This relation also holds between Hβ FWHM and λ5100 Å luminosity during disk-dominated phases, suggesting that the emission line arises mostly from the canonical virialized BLR. Moreover, jet-related λ5100 Å flares coincide with Hβ flares, suggesting the jet base lies within the BLR. From 219 disk-dominated spectra, we estimate a mean black hole mass of $M_{BH} = (2.85 \pm 0.37) \times 10^8\ M_\odot$. This study sheds light on the jet-BLR connection in PKS 1510-089, enhancing our understanding of blazar emission.

Key words: active galactic nuclei (16) – galaxy jets (601) – emission line galaxies (459) – flat-spectrum radio quasars (2163) – supermassive black holes (1663)

1. Introduction

PKS 1510-089 (redshift $z = 0.361$; Burbidge & Kinman, 1966) is a flat-spectrum radio quasar (FSRQ), one of the most active and well-studied sources across the entire electromagnetic spectrum (e.g. Marscher et al., 2010; Rani et al., 2010; Aleksić et al., 2014; Fuhrmann et al., 2016; Prince et al., 2019; Yuan et al., 2023). The relativistic jet of PKS 1510-089 is oriented at an angle of roughly 3° to our line of sight (Homan et al., 2002), allowing the detection of knots with apparent superluminal velocities of up to $20c$ along the jet (Jorstad et al., 2005). The location of the γ-ray emission zone in this source remains uncertain. Some studies place it close to the supermassive black hole (SMBH), within the broad-line region (BLR) (e.g. Poutanen & Stern, 2010; Tavecchio et al., 2010; Brown, 2013), while others argue for a position further downstream, beyond the BLR and outside the central parsec (e.g. Tavecchio et al., 2010; Orienti et al., 2013; Dotson et al., 2015; H.E.S.S. Collaboration et al., 2021). This complicates the identification of the dominant γ-ray production mechanism. While combined external Compton (EC) and synchrotron self-Compton (SSC) scenarios are often invoked (Kataoka et al., 2008; D'Ammando et al., 2009; Castignani et al., 2017), purely EC or SSC models (Aleksić et al., 2014; H.E.S.S. Collaboration et al., 2021) and lepto-hadronic interpretations (Dzhatdoev et al., 2022) have also been proposed and cannot be completely ruled out.

Aharonian et al. (2023) showed that during 2021 to 2022, PKS 1510-089 remained in a low activity state, accompanied by a decline in optical polarization, with spectra consistent with emission from the accretion disk and BLR. In these epochs, Barnard et al. (2024) reported that the strength and width of emission features (Mg II λ2798 Å, Hδ, and Hγ) were stable, but their average EW increased. Furthermore, Podjed et al. (2024) found no polarized broad Hγ or Hβ emission, suggesting that these lines are intrinsically unpolarized. Estimates of the black hole mass (M_{BH}) in PKS 1510-089 span a range of values. Disk temperature profile modeling yields values of 5.40 and 2.40×10^8 $M_\odot$ (Abdo et al., 2010; Castignani et al., 2017, respectively). Single-epoch spectra based on λ5100 Å continuum luminosity and Hβ full width at half maximum (FWHM) give values of 3.86 and 2.00×10^8 $M_\odot$ (Oshlack et al., 2002; Xie et al., 2005, respectively), while reverberation mapping by Rakshit (2020) yields a mass of $5.71^{+0.62}_{-0.58} \times 10^7$ $M_\odot$.

This work summarizes the results in Amador-Portes et al. (2024b, 2025), where γ-ray variability alongside the fluxes of Hβ and Hγ, the Hβ FWHM, and the optical continuum flux at λ5100 Å were analyzed. Multi-wavelength light curves spanning ~ 10 years using cross-correlation analysis were used to probe time lags between bands and infer the locations and dominant mechanisms of different emission regions. We also studied correlations between $L_{\lambda 5100}$ and $L_{\mathrm{H}\beta}$, as well as between FWHM Hβ and these luminosities. To assess the influence of the jet on BLR emission, we separated spectra based on the dominant continuum source, accretion disk or jet. For disk-dominated spectra, we estimated the MBH

via single-epoch methods from $L_{H\beta}$ and FWHM Hβ. Throughout this work, we adopt a cosmology with $H_0 = 71$ km s^{-1} Mpc^{-1}, $\Omega_\Lambda = 0.73$, and $\Omega_M = 0.27$, corresponding to a luminosity distance of 1906.9 Mpc at $z = 0.361$.

2. Observations and data

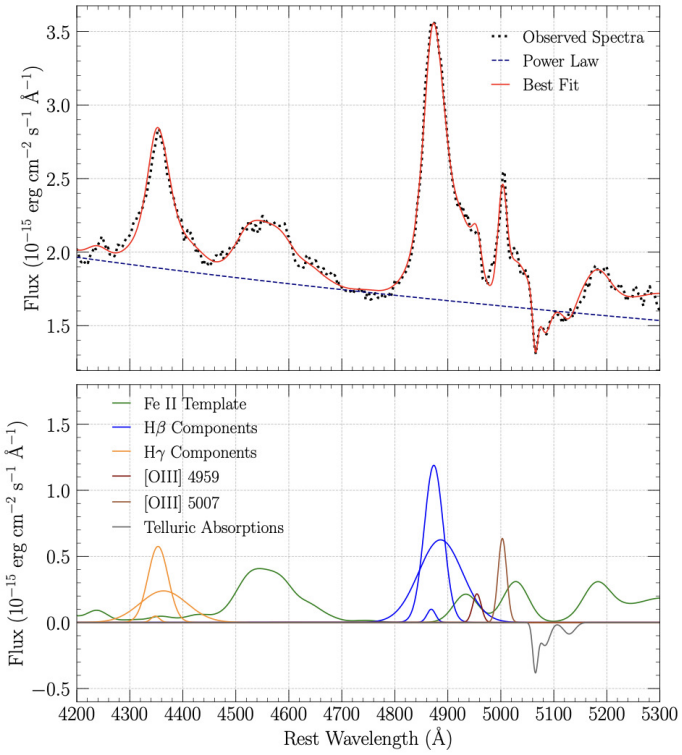

Figure 1. Example decomposition of the Hβ and Hγ emission lines from a spectrum observed at the Steward Observatory on April 10, 2018. Top panel: The rest-frame spectrum with the best-fit model overlaid. The continuum is represented by a power-law function. Bottom panel: The broad and narrow components used to fit Hβ and Hγ, along with the Fe II template, [O III] doublet, and telluric absorptions.

We analyzed γ-ray data ($0.1 - 300$ GeV) from the Fermi-LAT (Abdo et al., 2010) public archive[1] using `Fermitools version 2.0.8` to construct weekly light curves. The near-infrared (NIR) J-band data were obtained from the Small

[1] https://fermi.gsfc.nasa.gov/cgi-bin/ssc/LAT/LATDataQuery.cgi

and Moderate Aperture Research Telescope System (SMARTS; Bonning et al., 2012). Optical V-band data were retrieved from two sources, SMARTS and the Steward Observatory (SO). We obtained 34 optical spectra from the Observatorio Astrofísico Guillermo Haro (OAGH[2]), and 353 spectra from the SO as part of the Ground-based Observational Support of the Fermi Gamma-ray Space Telescope monitoring program at the University of Arizona[3]. The OAGH spectra, covers a wavelength range of 3800–7100 Å, while the SO spectra spans the wavelengths 4000–7500 Å. Details of the OAGH spectra data reduction is found in Amador-Portes et al. (2024b) and SO observational setup and data processing are provided in Smith et al. (2009).

The spectra were shifted to the rest frame and corrected for cosmological effects using the $(1+z)^3$ factor (Peterson, 1997). Galactic reddening was removed using the dust maps from Schlafly & Finkbeiner (2011) with $E(B-V) = 0.09$, adopting the reddening law of Cardelli et al. (1989) with $R_V = 3.1$. We extract the Hβ, Hγ, and λ5100 Å continuum fluxes through spectral decomposition. The local continuum was modeled with a power-law. Fe II multiplet emission between 4000–5500 Å was modeled using the template from Kovačević et al. (2010). Emission and absorption lines were fitted using the `astropy.modeling`[4] framework. The Hβ and Hγ lines were each fitted with three Gaussian components: narrow, broad, and very broad. An example of the spectral decomposition is shown in Figure 1.

Three sources of uncertainty were considered for the emission line flux measurements: i) Random error from spectral dispersion and signal-to-noise (S/N) ratio (Tresse et al., 1999); ii) uncertainties from Fe II subtraction (León-Tavares et al., 2013); and iii) a 10% contribution from flux calibration (Paul Smith private communication). The narrow Hβ contribution to the total profile was minimal, ranging from 5.2% at its lowest line flux to 1.5% at its highest line flux, smaller than the total Hβ flux uncertainty. Therefore, the total Hβ profile was used in all calculations. Given that the Hγ line is expected to behave similarly, its total profile flux was also adopted for the cross-correlation analysis.

We measured the FWHM from the sum of Gaussians used for the Hβ profile. The uncertainty in the observed FWHM arises from two sources: i) the random error due to spectral dispersion (~ 4 Å), and ii) the fitting error, estimated as the standard deviation between the fitted Gaussians and the observed spectrum. A correction by instrumental broadening was made for each slit width used in the SO observations, adopting the values from Amador-Portes et al. (2024a): 9.45 ± 2.70 Å for $3\farcs0$, 12.92 ± 3.69 Å for $4\farcs1$, and 16.07 ± 4.59 Å for $5\farcs1$. As the instrumental uncertainties dominate over S/N effects, the corrected FWHM was obtained via quadratic subtraction of the instrumental and observed profiles, with its uncertainty derived through standard error propagation.

[2] https://astro.inaoep.mx/observatorios/oagh/

[3] http://james.as.arizona.edu/~psmith/Fermi/

[4] https://docs.astropy.org/en/stable/modeling/index.html

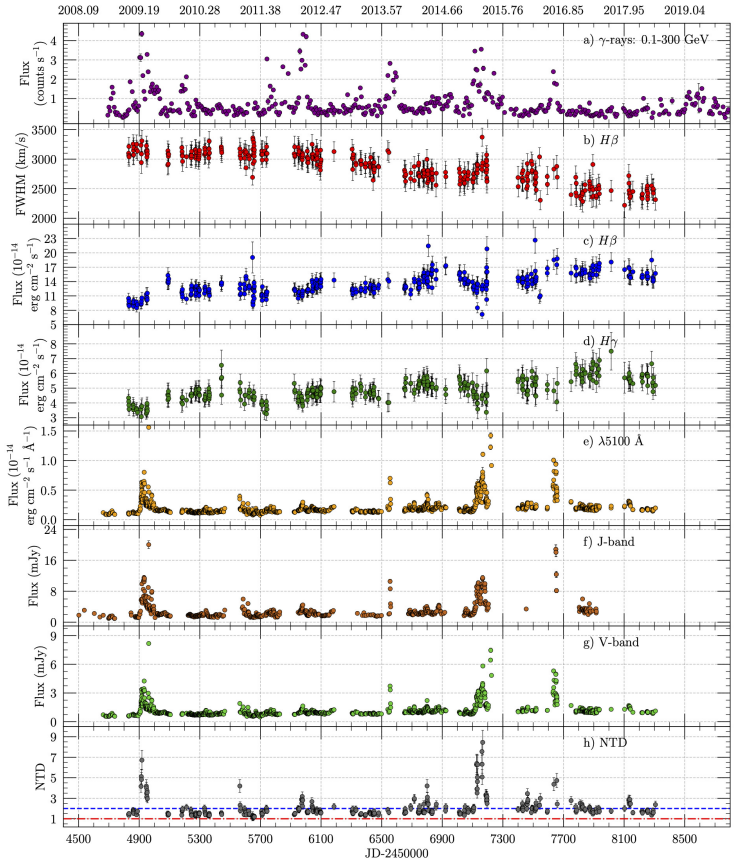

Figure 2. Multi-wavelength light curves. (a) γ-ray data from Fermi/LAT ($0.1 - 300$ GeV), (b) FWHM of the Hβ emission line, (c) Hβ emission line flux, (d) Hγ emission line flux, (e) λ5100 Å continuum flux, (f) V-band from SO and SMARTS, (g) J-band from SMARTS, and (h) NTD parameter. The red dash-dotted and blue dashed lines in panel (h) represent NTD= 1 and NTD= 2, respectively.

$$NTD = \frac{L_{obs}}{L_{pred}} \tag{1}$$

The NTD parameter (Shaw et al., 2012) was calculated following Equation 1, where $L_{\rm obs}$ is the observed continuum luminosity, and $L_{\rm pred}$ is the continuum luminosity predicted from the Hβ luminosity using the non-blazar relation of Greene & Ho (2005). The NTD parameter quantifies the relative non-thermal (jet) contribution to the total continuum emission in AGN. Following Patiño-Álvarez et al. (2016), NTD = 1 indicates purely thermal emission from the

accretion disk; $1 < \mathrm{NTD} < 2$ implies disk-dominated emission with a jet contribution; $\mathrm{NTD} = 2$ corresponds to equal contributions from disk and jet; and $\mathrm{NTD} > 2$ indicates jet-dominated emission. Thus, two regimes can be defined: Disk-Dominated ($\mathrm{NTD} < 2$) and Jet-Dominated ($\mathrm{NTD} > 2$). The light curves of the γ-rays, Hβ and λ5100 Å continuum fluxes along with the FWHM of Hβ and NTD are displayed in Figure 2.

3. Variability and correlations analysis

Table 1. Time lags between emission in different bands, and NTD values, obtained from cross-correlation analysis of the full light curves.

Light Curves	Delay (days)
5100 Åvs γ-rays	-6.8 ± 6.4
5100 Åvs Hβ	82.4 ± 6.1
5100 Åvs Hγ	87.7 ± 6.6
5100 Åvs J-band	0.0 ± 3.7
5100 Åvs NTD	0.1 ± 6.7
5100 Åvs V-band	0.2 ± 2.5
γ-rays vs NTD	6.0 ± 6.7
J-band vs γ-rays	-8.8 ± 6.4
J-band vs Hβ	81.8 ± 6.1
J-band vs NTD	-0.5 ± 6.7
V-band vs γ-rays	-9.0 ± 11.3
V-band vs Hβ	$78.9^{+14.9}_{-4.2}$
V-band vs J-band	0.0 ± 3.7
V-band vs NTD	0.6 ± 6.7

We conducted cross-correlations amongst all multi-wavelength light curves previously described. Three different methods were employed to ensure robustness: the interpolated cross-correlation function (ICCF; Gaskell & Sparke, 1986), the discrete cross-correlation function (DCCF; Edelson & Krolik, 1988), and the Z-transformed discrete cross-correlation function (ZDCF; Alexander, 1997). These methods followed the established protocols outlined in Patiño-Álvarez et al. (2013); Patiño-Álvarez et al. (2018), and Amaya-Almazán et al. (2022). Only time delays with correlation coefficients at above 99% significance,, and consistent across at least two of the three methods, were considered. Further details on significance levels can be found in Emmanoulopoulos et al. (2013) and Amaya-Almazán et al. (2022) The reported delays represent the average results obtained from either two or all three methods, depending on the case, with the reported uncertainty being the maximum uncertainty value among the

three methods employed. Results of the cross-correlation analysis for the are summarized in Table 1.

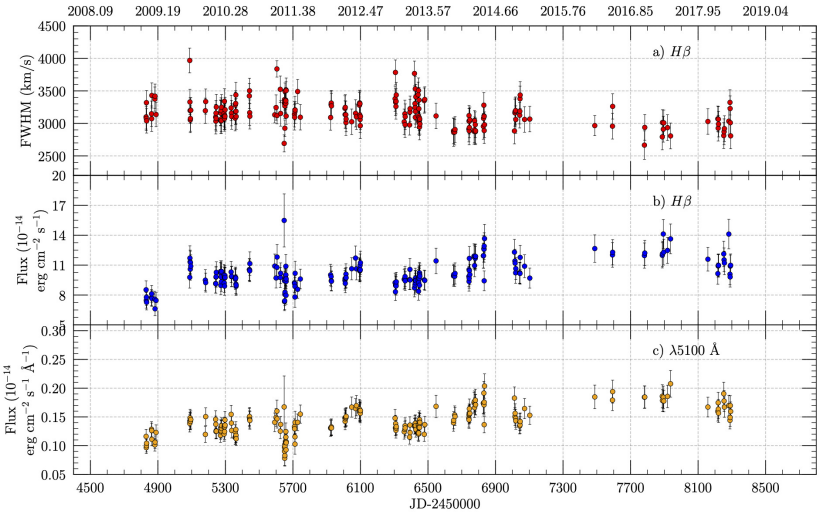

Figure 3. Spectroscopic light curves for the disk dominance regime. (a) FWHM of the Hβ emission line, (b) Hβ emission line flux, and (c) the λ5100 Å continuum flux.

Delays between the optical/NIR emissions (λ5100 Å continuum, J-band, V-band, and NTD) are consistent with zero, indicating quasi-simultaneous, co-spatial emission. Continuum variability is largely driven by flare-like episodes linked to strong jet activity, as shown by NTD values exceeding 2. Thus, the variability in the λ5100 Å continuum is predominantly powered by synchrotron emission from the jet. Given the co-spatiality, the V-band and J-band emissions during flares also arise primarily within the jet, confirming synchrotron radiation as the main driver of variability across these bands. The ∼80-day delay between the continuum and emission lines likely reflects the light-travel time from the continuum source to the BLR. In addition, a cross-correlation analysis between the λ5100 Å continuum and Hβ light curves, separated by jet- and disk-dominated regimes (NTD+σ $<$ 2) was performed. The results for these subsets did not reveal any significant correlation, indicating no physical delay between the light curves in separated regimes. In the jet dominance regime, the observed delays appeared to be spurious correlations. Conversely, in the disk dominance regime, we obtain inconclusive results, stemmed from the similarity in the light curves, characterized by prolonged periods of quiescence with minimal variability as shown in Figure 3. A detailed discussion of this inconclusive results is presented on Amador-Portes et al. (2024b).

Table 2. Pearson (ρ_P) and Spearman (ρ_S) correlation coefficients obtained for $L_{\lambda 5100}$ versus $L_{H\beta}$ and $L_{H\beta}$ or $L_{\lambda 5100}$ versus $FWHM_{H\beta}$ across various data sets: Full Set, Disk Dominance (DD), and Jet Dominance (JD). Corresponding p-values are displayed for each case.

Regime	ρ_P	p_v	ρ_S	p_v
		$L_{\lambda 5100}$ vs $L_{H\beta}$		
Full Set	0.200	2.60×10^{-6}	0.450	6.0×10^{-21}
DD	0.800	6.90×10^{-59}	0.810	7.00×10^{-53}
JD	0.100	0.260	0.170	0.200
		$L_{\lambda 5100}$ vs $FWHM_{H\beta}$		
Full Set	-0.187	2.09×10^{-4}	-0.450	2.27×10^{-20}
DD	-0.678	8.81×10^{-31}	-0.650	6.21×10^{-28}
JD	-0.104	0.395	-0.054	0.658
		$L_{H\beta}$ vs $FWHM_{H\beta}$		
Full Set	-0.650	9.34×10^{-48}	-0.683	1.72×10^{-54}
DD	-0.678	8.04×10^{-31}	-0.651	7.86×10^{-28}
JD	-0.575	2.33×10^{-7}	-0.630	6.59×10^{-9}

The delay of 7.0 ± 7.7 days between optical/NIR bands and γ-ray emission suggests that the optical emission region and the source of seed photons are quasi-cospatial. Since optical variability is jet-driven, delays between the optical light curves and other light curves will also trace jet activity during flares. The near-zero lag therefore indicates that optical/NIR and γ-ray emission regions are co-spatial within the jet. For the γ-ray energies detected by Fermi/LAT (0.1−300 GeV), the seed photons must be within the NIR-NUV range, corresponding to observable flux in the V-band, J-band, and $\lambda 5100$ Å continuum. Given the quasi-cospatiality of optical/NIR and seed photon regions within the jet, SSC is favored as the dominant emission mechanism during flares, where γ-rays arise from synchrotron photons scattered by the same relativistic electrons. However, EC processes cannot be excluded, as both are expected to occur simultaneously.

We look for correlations in the logarithmic space between $FWHM_{H\beta}$, $L_{\lambda 5100}$, and $L_{H\beta}$ for the entire dataset, as well as separately for the jet dominance and disk dominance regimes to picture the role of jet emission over the Hβ emission line (and thus the BLR). The correlations were conducted with the Pearson (ρ_P) and Spearman (ρ_S) correlation rank tests, Person or Spearman coefficients with values absolute below $|\rho| \leq 0.39$ are considered as a weak correlation, values between $0.40 \leq |\rho| \leq 0.59$ as a moderate correlation, and values greater than $|\rho| \geq 0.60$ as a strong correlation (positive or negative, given the case). All correlation coefficients are displayed in Table 2.

$$L_{\lambda 5100} = 10^{44}\ \mathrm{erg\ s^{-1}} \left(\frac{L_{H\beta}}{(1.425 \pm 0.007) \times 10^{42}\ \mathrm{erg\ s^{-1}}} \right)^{-\frac{1}{1.133 \pm 0.005}} \quad (2)$$

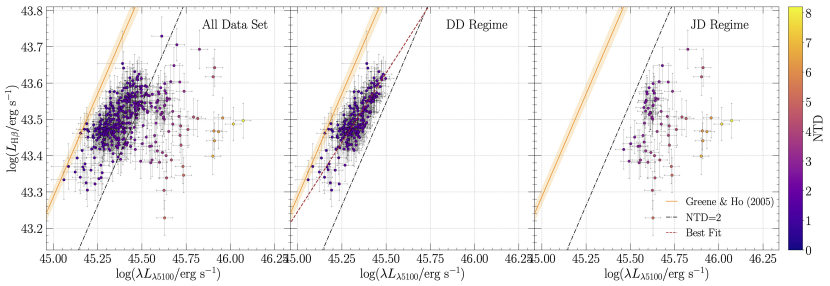

Figure 4. Variation of the Hβ emission-line luminosity compared to the λ5100 Å continuum luminosity. In all panels, the color bar indicates the NTD value for each observation. Left Panel: Full sample. Middle Panel: Disk dominance (DD) regime data. Right Panel: Jet dominance (JD) regime data. The dashed black line denotes the boundary between the regimes. The orange solid line and shaded area represent the Greene & Ho (2005) relation for a non-blazar sample and its uncertainty at 3σ. The dashed red line denotes the significant ($p_v < 0.05$) linear regression to the correspondent data.

The NTD parameter, defined as the ratio of observed to predicted continuum luminosity, with predictions based on the Hβ - continuum relation (Equation 2) from Greene & Ho 2005, was used to distinguish between jet- and disk-dominated states. Figure 4 shows this comparison, with NTD= 2 marking the boundary. Across the full sample, correlations between continuum and Hβ luminosities were weak to moderate, and linear regression failed to yield a significant fit (as evidenced by their p-value[5], p_v of 1 to machine accuracy). For the linear regression, a p-value below 0.05 is considered statistically significant, indicating that the observed relationship is unlikely to have occurred by chance. To refine the analysis, we separated the data: 219 spectra (56.6%) in the disk-dominated regime, 17.8% in the jet-dominated regime, and 25.6% near the threshold. In the disk-dominated regime, a strong correlation was recovered, with a slope of $\beta = 0.76 \pm 0.05$ ($p_v \approx 0$) for the linear regression, consistent with a non-blazar AGN. In contrast, no significant correlation was found in the jet-dominated regime, indicating that line luminosities do not reliably track continuum variability when the jet dominates.

Across the full dataset, the Pearson test shows no correlation between $L_{\lambda 5100}$ and FWHM$H\beta$, while the Spearman test reveals a moderate anti-correlation, indicating a monotonic but non-linear relationship; the linear regression does not accurately describe the data ($p_v = 0.620$). In the disk-dominated regime, strong correlations appear in both tests, with a regression slope $\beta = -0.360 \pm 0.034$ ($p_v \approx 0.0$), reflecting the "breathing-BLR" effect (Figure 5): as the ionizing

[5]The p-value represents the probability that our null hypothesis is true, which states there is no relationship between the model and the data.

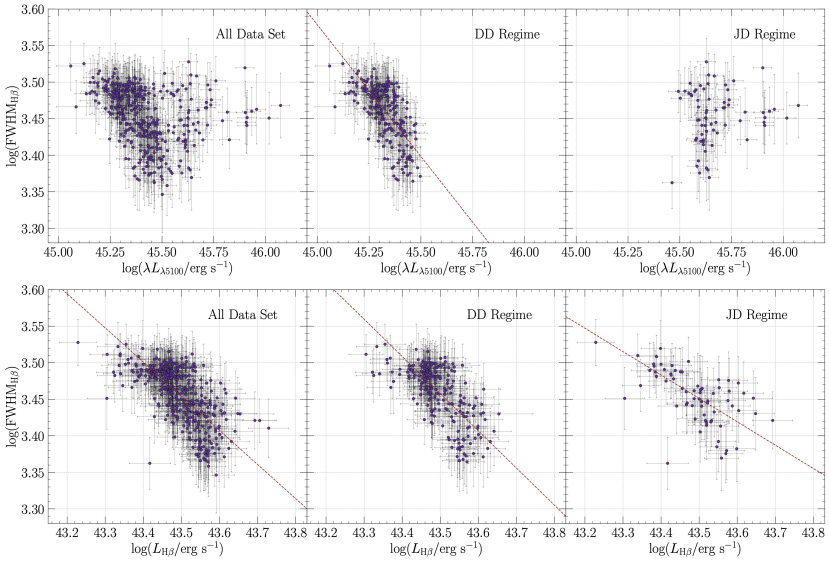

Figure 5. Top Row: Variation of the Hβ emission-line FWHM compared to the λ5100 Å continuum luminosity. Bottom Row: Variation of the Hβ emission-line FWHM compared to its luminosity. Left Column: Full sample. Middle Column: Disk dominance (DD) regime data set. Right Column: Jet dominance (JD) regime data set. Only linear regression fits with $p_v < 0.05$ are plotted, as red dashed lines, for the corresponding data.

continuum increases, the BLR radius expands due to clouds farther away being ionized, producing narrower Hβ profiles. In contrast, the jet-dominated regime shows no significant correlation, implying that the ionizing influence of the jet on the BLR is weaker compared to the accretion disk, thus insufficient to induce a similar dynamic response in the BLR. We find a strong anti-correlation between $L_{H\beta}$ and FWHM$_{H\beta}$ across all subsets, indicating that changes in Hβ luminosity similarly affect the BLR regardless of the ionizing source. Long-term trends over $\sim$ 10 years show that flux increases correspond to FWHM decreases. Linear regression is statistically significant for all subsets, with slopes $\beta = -0.467 \pm 0.032$ (full dataset), $\beta = -0.509 \pm 0.048$ (disk-dominated), and $\beta = -0.320 \pm 0.056$ (jet-dominated), all with $p_v < 0.002$.

The observed "breathing-BLR" effect, indicates that the photons driving the Hβ emission consistently originate from the canonical BLR, regardless of whether the dominant continuum source is the accretion disk or the jet. This rules out the contribution of any external BLR material. Based on these, we propose that the base of the jet, where the UV synchrotron emission is produced, resides within the canonical BLR. In this configuration, the jet emission directly

impacts the Hβ line, reinforcing the idea that the canonical BLR remains the principal emission region even when the jet dominates the continuum. In Figure 6 we present a schematic illustration of the Jet-BLR system coupling and the different interactions between regions.

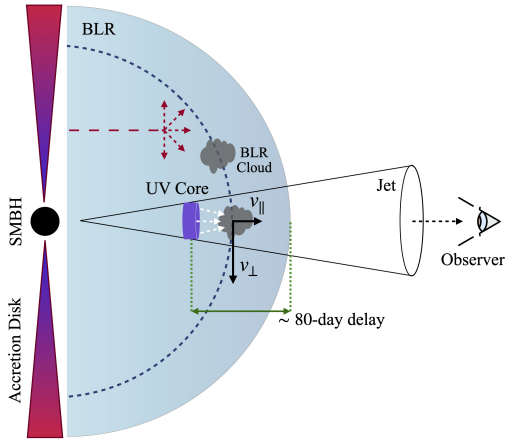

Figure 6. Schematic illustration of the Jet-BLR system suggested in this work (not to scale). The blue dashed curve represents the orbit of a BLR cloud around the SMBH with the parallel velocity component being low while crossing the jet section. BLR clouds in this region will be ionized by a contribution of UV flux from the accretion disk (red arrows) and from the jet (white arrows). The $\sim$ 80-day delay between the continuum emission and the Hβ emission line traces the distance between the continuum emission within the jet during flare-like events and the edge of the BLR.

4. Black hole mass estimation

The variability in this source is predominantly jet-driven. This complicates supermassive black hole mass (M_{BH}) estimates via reverberation mapping, since the measured delay in disk dominance regime yielded inconclusive results we could not use reverberation mapping. Given these limitations, we adopted single-epoch spectroscopic methods for M_{BH} estimation, applying Equation 3 from Greene & Ho (2005) to 192 spectra in the disk-dominated regime. FWHM$_{H\beta}$ is corrected for instrumental broadening. From this set of data points, we estimated a weighted mean mass for the supermassive black hole (M_{BH}). The resulting value is $M_{BH} = 2.85 \pm 0.37 \times 10^8\ M_{\odot}$, with the uncertainty derived from the standard deviation of this set.

$$M_{\rm BH} = (3.6 \pm 0.2) \times 10^6 \left(\frac{L_{H\beta}}{10^{42}\ {\rm erg/s}} \right)^{0.56\pm0.02} \left(\frac{FWHM_{H\beta}}{10^3\ {\rm km/s}} \right)^2 M_\odot \qquad (3)$$

5. Summary and results

Delays between optical/IR emissions are consistent with zero, indicating nearly simultaneous, co-spatial regions. Continuum variability is driven by flares, suggesting that optical and NIR emissions mainly arise from synchrotron processes in the jet. The 7.0 ± 7.7-day lag between optical/IR and γ-rays indicates a close spatial link, with seed photons for inverse Compton emission originating from jet-produced optical/NIR flux. SSC is suspected to be the dominant γ-ray emission process during flare-like events, but further analysis needs to be made. Cross-correlations across the full dataset between the λ5100 Å continuum and the Hβ and Hγ emission line fluxes revealed a delay of approximately 80 ± 6 days. This delay reflects the separation between the continuum emission region and the BLR, and cannot be interpreted as the size of a virialized BLR. Instead, it likely traces the distance between the edge of the BLR and the continuum source associated with the jet during flare-like events. In the disk-dominated regime, the results were inconclusive, a behavior attributed to the prevalence of quiescent periods with minimal variability.

The λ5100 Å continuum and Hβ luminosities show a weak positive correlation across the full dataset, diverging from the non-blazar relation at NTD> 2. In the disk dominance regime, the correlation strengthens (Pearson $= 0.80$, Spearman $= 0.79$), indicating that the emission line closely follows the continuum, as in non-blazar AGNs. A consistent anti-correlation between $L_{H\beta}$ and FWHM$_{H\beta}$ across all datasets reflects the "breathing-BLR" effect. These results suggest that the BLR responds similarly to ionizing flux from both the accretion disk and the jet, supporting a scenario where the jet base is embedded within the canonical BLR.

Single-epoch spectra were employed to estimate M_{BH} in the disk dominance regime, using the scaling relation proposed by Greene & Ho (2005). A robust M_{BH} value of $2.85 \pm 0.37 \times 10^8\ M_\odot$ was derived exclusively from spectra spanning approximately a decade within the disk dominance regime. This approach minimized jet contamination and short-term variability potentially associated with jets. However, for this object, the jet does not significantly impact the M_{BH} estimated, as seen from the analysis of the complete spectra set for this particular source.

Acknowledgements. A.A.-P. and A. G.-P. gratefully acknowledges the support received from the SECIHTI (Secretaria de Ciencias, Humanidades, Tecnología e Inovación) program for their Ph.D. studies. This work was made possible thanks to the generous assistance provided by the Max Planck Institute for Radio Astron-

omy (MPIfR) - Mexico Max Planck Partner Group led by V.M.P.-A. Data from the Steward Observatory spectropolarimetric monitoring project were used. This program is supported by Fermi Guest Investigator grants NNX08AW56G, NNX09AU10G, NNX12AO93G, and NNX15AU81G. This publication is based on data collected at the Observatorio Astrofísico Guillermo Haro (OAGH), Cananea, Sonora, Mexico, operated by the Instituto Nacional de Astrofísica, Óptica y Electrónica (INAOE). Funding for the OAGH has been provided by SECIHTI.

References

Abdo, A. A., Ackermann, M., Agudo, I., et al., FERMI LARGE AREA TELESCOPE AND MULTI-WAVELENGTH OBSERVATIONS OF THE FLARING ACTIVITY OF PKS 1510-089 BETWEEN 2008 SEPTEMBER AND 2009 JUNE. 2010, *The Astrophysical Journal*, **721**, 1425, DOI:10.1088/0004-637X/721/2/1425

Aharonian, F., Benkhali, F. A., Aschersleben, J., et al., The Vanishing of the Primary Emission Region in PKS 1510–089. 2023, *The Astrophysical Journal Letters*, **952**, L38, DOI:10.3847/2041-8213/ace3c0

Aleksić, J., Ansoldi, S., Antonelli, L. A., et al., MAGIC gamma-ray and multi-frequency observations of flat spectrum radio quasar PKS 1510-089 in early 2012. 2014, *A&A*, **569**, A46, DOI:10.1051/0004-6361/201423484

Alexander, T., Is AGN Variability Correlated with Other AGN Properties?—ZDCF Analysis of Small Samples of Sparse Light Curves. 1997, in *Astronomical Time Series*, ed. D. Maoz, A. Sternberg, & E. M. Leibowitz (Dordrecht: Springer Netherlands), 163–166

Amador-Portes, A., Chavushyan, V., & Patiño-Álvarez, V. M., Instrumental Broadening of the SPOL Spectropolarimeter at the University of Arizona. 2024a, *Revista Mexicana de Astronomia y Astrofisica*, **60**, 317, DOI:10.22201/ia.01851101p.2024.60.02.09

Amador-Portes, A., Chavushyan, V., Patiño-Álvarez, V. M., & Ramón-Valdés, J., Unveiling the Emission Mechanisms of Blazar PKS 1510-089. II. Jet-BLR Connection and Black Hole Mass Estimation. 2025, *Astrophysical Journal*, **979**, 227, DOI:10.3847/1538-4357/ada38b

Amador-Portes, A., García-Pérez, A., Chavushyan, V., & Patiño-Álvarez, V. M., Unveiling the Emission Mechanisms of Blazar PKS 1510-089. I. Multiwavelength Variability. 2024b, *Astrophysical Journal*, **977**, 178, DOI:10.3847/1538-4357/ad8ddd

Amaya-Almazán, R. A., Chavushyan, V., & Patiño-Álvarez, V. M., Multiwavelength Analysis and the C iv λ 1549 Å Emission Line Behavior From 2008 to 2020 of FSRQ B2 1633+382. 2022, *The Astrophysical Journal*, **929**, 14, DOI:10.3847/1538-4357/ac5741

Barnard, J., van Soelen, B., Acharya, S., et al., The optical spectropolarimetric behaviour of a selection of high-energy blazars. 2024, *Monthly Notices of the RAS*, **532**, 1991, DOI:10.1093/mnras/stae1576

Bonning, E., Urry, C. M., Bailyn, C., et al., SMARTS OPTICAL AND INFRARED MONITORING OF 12 GAMMA-RAY BRIGHT BLAZARS. 2012, *The Astrophysical Journal*, **756**, 13, DOI:10.1088/0004-637X/756/1/13

Brown, A. M., Locating the γ-ray emission region of the flat spectrum radio quasar PKS 1510-089. 2013, *Monthly Notices of the RAS*, **431**, 824, DOI:10.1093/mnras/stt218

Burbidge, E. M. & Kinman, T. D., Redshifts of Fourteen Quasi-Stellar Radio Sources. 1966, *Astrophysical Journal*, **145**, 654, DOI:10.1086/148808

Cardelli, J. A., Clayton, G. C., & Mathis, J. S., The Relationship between Infrared, Optical, and Ultraviolet Extinction. 1989, *Astrophysical Journal*, **345**, 245, DOI:10.1086/167900

Castignani, G., Pian, E., Belloni, T. M., et al., Multiwavelength variability study and search for periodicity of PKS 1510-089. 2017, *A&A*, **601**, A30, DOI:10.1051/0004-6361/201629775

D'Ammando, F., Pucella, G., Raiteri, C. M., et al., AGILE detection of a rapid flare from the blazar PKS 1510-089 during the GASP-WEBT monitoring*. 2009, *A&A*, **508**, 181, DOI:10.1051/0004-6361/200912560

Dotson, A., Georganopoulos, M., Meyer, E. T., & McCann, K., On the Location of the 2009 GeV Flares of Blazar PKS 1510-089. 2015, *Astrophysical Journal*, **809**, 164, DOI:10.1088/0004-637X/809/2/164

Dzhatdoev, T. A., Khalikov, E. V., Latypova, V. S., Podlesnyi, E. I., & Vaiman, I. A., Modeling the persistent low-state gamma-ray emission of the PKS 1510-089 blazar with electromagnetic cascades initiated in hadronuclear interactions. 2022, *Monthly Notices of the Royal Astronomical Society*, **515**, 5242, DOI:10.1093/mnras/stac2094

Edelson, R. A. & Krolik, J. H., The Discrete Correlation Function: A New Method for Analyzing Unevenly Sampled Variability Data. 1988, *Astrophysical Journal*, **333**, 646, DOI:10.1086/166773

Emmanoulopoulos, D., McHardy, I. M., & Papadakis, I. E., Generating artificial light curves: revisited and updated. 2013, *Monthly Notices of the RAS*, **433**, 907, DOI:10.1093/mnras/stt764

Fuhrmann, L., Angelakis, E., Zensus, J. A., et al., The F-GAMMA programme: multi-frequency study of active galactic nuclei in the Fermi era. Programme description and the first 2.5 years of monitoring. 2016, *Astronomy and Astrophysics*, **596**, A45, DOI:10.1051/0004-6361/201528034

Gaskell, C. M. & Sparke, L. S., Line Variations in Quasars and Seyfert Galaxies. 1986, *Astrophysical Journal*, **305**, 175, DOI:10.1086/164238

Greene, J. E. & Ho, L. C., Estimating Black Hole Masses in Active Galaxies Using the Hα Emission Line. 2005, *The Astrophysical Journal*, **630**, 122, DOI:10.1086/431897

H.E.S.S. Collaboration, Abdalla, H., Adam, R., et al., H.E.S.S. and MAGIC observations of a sudden cessation of a very-high-energy flare in PKS 1510-089 in May 2016. 2021, *A&A*, **648**, A23, DOI:10.1051/0004-6361/202038949

Homan, D. C., Wardle, J. F. C., Cheung, C. C., Roberts, D. H., & Attridge, J. M., PKS 1510–089: A Head-on View of a Relativistic Jet. 2002, *The Astrophysical Journal*, **580**, 742, DOI:10.1086/343894

Jorstad, S. G., Marscher, A. P., Lister, M. L., et al., Polarimetric Observations of 15 Active Galactic Nuclei at High Frequencies: Jet Kinematics from Bimonthly Monitoring with the Very Long Baseline Array. 2005, *Astronomical Journal*, **130**, 1418, DOI:10.1086/444593

Kataoka, J., Madejski, G., Sikora, M., et al., Multiwavelength Observations of the Powerful Gamma-Ray Quasar PKS 1510–089: Clues on the Jet Composition. 2008, *The Astrophysical Journal*, **672**, 787, DOI:10.1086/523093

Kovačević, J., Popović, L. Č., & Dimitrijević, M. S., Analysis of Optical Fe II Emission in a Sample of Active Galactic Nucleus Spectra. 2010, *Astrophysical Journal, Supplement*, **189**, 15, DOI:10.1088/0067-0049/189/1/15

León-Tavares, J., Chavushyan, V., Patiño-Álvarez, V. M., et al., Flare-like Variability of the Mg II λ2800 Emission Line in the γ-ray Blazar 3C 454.3. 2013, *The Astrophysical Journal Letters*, **763**, L36, DOI:10.1088/2041-8205/763/2/L36

Marscher, A. P., Jorstad, S. G., Larionov, V. M., et al., PROBING THE INNER JET OF THE QUASAR PKS 1510-089 WITH MULTI-WAVEBAND MONITORING DURING STRONG GAMMA-RAY ACTIVITY. 2010, *The Astrophysical Journal Letters*, **710**, L126, DOI:10.1088/2041-8205/710/2/L126

Orienti, M., Koyama, S., D'Ammando, F., et al., Radio and γ-ray follow-up of the exceptionally high-activity state of PKS 1510-089 in 2011. 2013, *Monthly Notices of the RAS*, **428**, 2418, DOI:10.1093/mnras/sts201

Oshlack, A. Y. K. N., Webster, R. L., & Whiting, M. T., Black Hole Mass Estimates of Radio-selected Quasars. 2002, *The Astrophysical Journal*, **576**, 81, DOI:10.1086/341729

Patiño-Álvarez, V. M., Carramiñana, A., Carrasco, L., & Chavushyan, V., A Multiwavelength Cross-Correlation Variability Study of Fermi-LAT Blazars. 2013, in *4th Fermi Symposium, eConf Proceedings C121028*, Monterey, CA, 0–6, 4th Fermi Symposium, eConf Proceedings C121028, 6 pages, 2 figures.

Patiño-Álvarez, V. M., Torrealba, J., Chavushyan, V., et al., Baldwin Effect and Additional BLR Component in AGN with Superluminal Jets. 2016, *Frontiers in Astronomy and Space Sciences*, **3**, 19, DOI:10.3389/fspas.2016.00019

Patiño-Álvarez, V. M., Fernandes, S., Chavushyan, V., et al., Multiwavelength photometric and spectropolarimetric analysis of the FSRQ 3C 279. 2018, *Monthly Notices of the Royal Astronomical Society*, **479**, 2037, DOI:10.1093/mnras/sty1497, _eprint: https://academic.oup.com/mnras/article-pdf/479/2/2037/25142034/sty1497.pdf

Peterson, B. M. 1997, *An Introduction to Active Galactic Nuclei*

Podjed, S. A., Hickox, R. C., Isler, J. C., Böttcher, M., & Schutte, H. M., Optical Spectropolarimetric Variability Properties in Blazars PKS 0637–75 and PKS 1510–089. 2024, *Astrophysical Journal*, **968**, 130, DOI:10.3847/1538-4357/ad4111

Poutanen, J. & Stern, B., GeV Breaks in Blazars as a Result of Gamma-ray Absorption Within the Broad-line Region. 2010, *Astrophysical Journal, Letters*, **717**, L118, DOI:10.1088/2041-8205/717/2/L118

Prince, R., Gupta, N., & Nalewajko, K., Two-zone Emission Modeling of PKS 1510-089 during the High State of 2015. 2019, *The Astrophysical Journal*, **883**, 137, DOI:10.3847/1538-4357/ab3afa

Rakshit, S., Broad line region and black hole mass of PKS 1510-089 from spectroscopic reverberation mapping. 2020, *A&A*, **642**, A59, DOI:10.1051/0004-6361/202038324

Rani, B., Gupta, A. C., Strigachev, A., et al., Short-term flux and colour variations in low-energy peaked blazars. 2010, *Monthly Notices of the RAS*, **404**, 1992, DOI:10.1111/j.1365-2966.2010.16419.x

Schlafly, E. F. & Finkbeiner, D. P., Measuring Reddening with Sloan Digital Sky Survey Stellar Spectra and Recalibrating SFD. 2011, *Astrophysical Journal*, **737**, 103, DOI:10.1088/0004-637X/737/2/103

Shaw, M. S., Romani, R. W., Cotter, G., et al., SPECTROSCOPY OF BROAD-LINE BLAZARS FROM 1LAC. 2012, *The Astrophysical Journal*, **748**, 49, DOI:10.1088/0004-637X/748/1/49

Smith, P. S., Montiel, E., Rightley, S., et al., Coordinated Fermi/Optical Monitoring of Blazars and the Great 2009 September Gamma-ray Flare of 3C 454.3. 2009, in *Fermi Symposium, eConf Proceedings C091122*, Washington, D.C, 0–6, 2009 Fermi Symposium, eConf Proceedings C091122, 6 pages, 2 figures.

Tavecchio, F., Ghisellini, G., Bonnoli, G., & Ghirlanda, G., Constraining the location of the emitting region in Fermi blazars through rapid γ-ray variability. 2010, *Monthly Notices of the RAS*, **405**, L94, DOI:10.1111/j.1745-3933.2010.00867.x

Tresse, L., Maddox, S., Loveday, J., & Singleton, C., Spectral analysis of the Stromlo-APM Survey — I. Spectral properties of galaxies. 1999, *Monthly Notices of the Royal Astronomical Society*, **310**, 262, DOI:10.1046/j.1365-8711.1999.02977.x

Xie, G. Z., Liu, H. T., Cha, G. W., et al., Spectrophotometry and Photometry for Five Blazars and Their Central Black Hole Masses. 2005, *Astronomical Journal*, **130**, 2506, DOI:10.1086/497163

Yuan, Q., Kushwaha, P., Gupta, A. C., et al., Multiwavelength Temporal Variability of the Blazar PKS 1510-089. 2023, *Astrophysical Journal*, **953**, 47, DOI:10.3847/1538-4357/acdd74